

# Stability, Current Drive and Heating, Energetic Particles: Summary Review<sup>1</sup>

K. Razumova

Russian Research Center, Kurchatov Institute, Moscow, Russian Federation

e-mail contact of author: razumova@nfi.kiae.ru

**Abstract.** The paper summarizes the results presented at the conference Fusion Energy 2000 (FEC 2000) in relation to the following subjects: 1. The possibility of realizing plasma parameters for ITER needs, advanced regimes in tokamaks and stellarators. 2. Stability of plasmas with an appreciable component of fast particles. 3. Low aspect ratio tokamaks. 4. New results with auxiliary heating and current drive methods. 5.  $\beta$  limit and neoclassical tearing mode (NTM) stabilization. 6. Internal transport barriers.

## 1. Advanced regimes

### 1.1. Tokamaks

The main goal of the experiments, whose results were presented at this Conference is to provide answers to ITER problems. These include: a) the possibility of operating at the upper limit of plasma parameters or even overcoming them; b) the possibility of maintaining these parameters stationary, c) obtaining total non-inductive plasma current with a high fraction of bootstrap current; d) then influence of energetic particles on the plasma stability and so on.

The results of the experiments are promising. As one can see in *FIG. 1*, which presents the results from one of the largest tokamaks, JT-60U, the plasma parameters in the same shot practically reach or even overcome the values determined by ITER needs. Promising results also were reported by other large tokamaks. The Greenwald density limit is exceeded in experiments on DIII-D, JET, JT-60U, ASDEX-U, TEXTOR and HT-7. The product of normalized beta,  $\beta_N$ , and confinement enhancement factor in relation to the ITER scaling (ITER89P),  $H_{89}$ , increases by up to a factor of 9 in DIII-D experiments with 75% of non-inductive current and a process duration  $\Delta t=16\tau_E$ . In JT-60U experiments the  $\beta_N \cdot H_{89}$  product was up to 7.2 for 1.5 MA of fully non-inductive current with a duration ( $\Delta t=2$  s) that many times exceeds the confinement time. In JET, ITER-like regimes with DT burning plasma

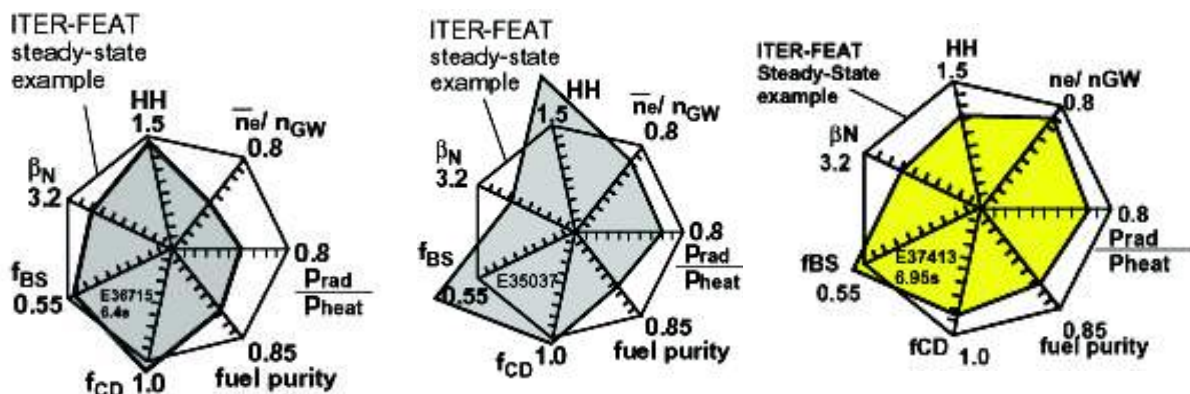


*FIG. 1. JT-60U. Achieved integrated performance relative to the target values in ITER-FEAT steady-state operation for three regimes: a) ELMy H-mode,  $q_{95}=4.75$ , full non-inductive current 1.5 MA; b) ELMy H-mode,  $q_{95}=9.3$ , full non-inductive current 0.8 MA; c) pellet fueled ELMy H-mode,  $q_{95}=6.5$ .*

<sup>1</sup> The issues of the plasma edge, divertor, H-mode and new theoretical results may be found in the review of Prof. F. Romanelli

were successfully investigated. It has been shown that the Greenwald density limit may be exceeded in a factor of 1.6, but with some deterioration of confinement.

Although the plasma parameters required for ITER were not reached simultaneously in any single experiment, present progress seems to leave no doubt that they can all be reached in the near future.

## 1.2. Stellarators

It is very interesting to note that plasma parameters in stellarators increase year by year, and now they have reached values typical for tokamaks. The experimentally measured tokamak and stellarator energy confinement times agree with the stellarator scaling ISS95 with the same accuracy. For the largest stellarator type device, LHD, the plasma parameters:  $T_e = 4.4$  keV,  $T_i = 3.5$  keV,  $n_e = 1.1 \times 10^{20} \text{ m}^{-3}$ ,  $\tau_E = 0.3$  s and  $\beta_T = 2.4\%$  are reached.

## 2. Fast particles

One of the most important problems for ITER is stability and confinement of  $\alpha$ -particles, which are the main source of the plasma heating power. Experiments in this area may be carried out either in a DT plasma or in a plasma with fast particles injected by neutral beams (NB) or generated during ICR heating. In such conditions the main expected instability is Toroidal Alfvén Eigenmodes (TAE). Its excitation requires a high ratio between the velocities of ions and Alfvén waves,  $v_{b\parallel}/v_A$ , and a sufficiently high normalized pressure of the fast ions,  $\beta_h$ . In START, ASDEX-U, DIII-D and JT-60U, the fast ions were generated by high energy neutral beam injection (NBI) or by tail particles born during ICR heating. In JT-60U the ion energy due to negative ion based neutral beam (N-NB) injection was up to 360 keV. Two kinds of instability were found and investigated: a low-frequency sweep and a high-frequency sweep. The latter develops during a short time (1–5 ms) and ends with an abrupt large amplitude event, leading to the loss of fast particles. The experiments were performed in the

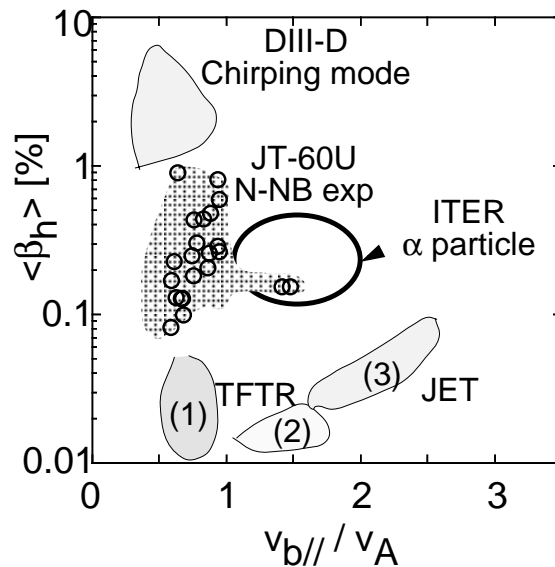


FIG. 2. Parameter domains in  $\langle \beta_h \rangle$  and  $v_{b\parallel}/v_A$  space of Alfvén Eigenmode experiments performed in large tokamaks. Open circles show JT-60U experiments that observed TAE instabilities with frequency sweeping by employing N-NB. An expected  $\alpha$ -particle parameter domain in ITER is also shown. A DIII-D fast ion parameter domain, where chirping modes with frequency sweeping in 1–10 ms were observed, and  $\alpha$ -particle parameter domains (1), (2) in TFTR DT experiments and (3) in JET DT experiments are presented. TAE were observed in (1) but not in (2) and (3).

region inside  $v_{b\parallel}/v_A \leq 1$ ,  $0.1\% < \beta_h < 1\%$  (FIG. 2). Close to this region in DIII-D experiments, the “chirping” Alfvén instability was found. It was shown that its appearance is connected with on-axis ICRF together with NBI heating. Off-axis ICRH and a low  $q$  edge value make it possible to avoid this kind of instability.

Investigation of the fast particle stability in DT plasma experiments was performed at TFTR (previously) and at JET. The region of these experiments may be seen in FIG. 2 in the  $\beta_h - v_{b\parallel}/v_A$  plane. There was no effect when the auxiliary heating method did not generate fast particles. In the latest JET experiments the increment predicted for TAEs by theory was verified by observing them in the presence of different fast particle sources. The saddle coil was used for exciting modes in the low-frequency MHD range. Looking at FIG. 2, we can say that in this area a lot of work remains to be done in order to answer the question of how  $\alpha$ -particles will be confined in ITER.

The theory presented at the Conference predicts that TAEs will appear in low aspect ratio tokamaks and also in stellarators. It seems that these modes will not lead to very dramatic consequences but scientists must be aware that attention may have to be given to this problem and that some special control of the radial parameter distribution may be required.

Relativistic electron beam generation is undesirable for a reactor. This problem was investigated in JET, JT-60U, TEXTOR and ASDEX-U experiments. Ways of terminating the electron beam are suggested. One of them is a large MHD spike with the toroidal mode number  $n=1$ .

### 3. Low aspect ratio tokamaks

This new branch of the tokamak family is developing quickly. Now at least 6 devices exist (see Table I). The START device operated during many years and its results are well known. NSTX and MAST have been operating for over a year and their results were presented at the Conference. A non-inductive start of discharge is realized by the “Coaxial Helicity Injection” (CHI) in NSTX. Plasma current  $I_p=1.1$  MA,  $k=2.5$  and  $\beta_t=6\%$  were reached in OH regimes. In experiments with NBI power  $P_{NB}=2.8$  MW,  $\beta_t$  increase was up to 22%, which means that normalized  $\beta_N=3.2$ . Another methods of heating/CD are planning in these tokamaks, including High Harmonic Fast Waves (HHFW). Experiments with  $q(r)$  control are beginning. In MAST, current  $I_p=1$  MA and electron temperature  $T_e=1$  keV are reached. Regimes with sawtooth and L-H transition, which are typical for conventional tokamaks, were obtained. The third new machine of this type, GLOBUS-M has begun operation. Current  $I_p=0.25$  MA, which is near the project value, has been achieved.

TAB I: LOW ASPECT RATIO DEVICES

Name	A	$I_p$ , MA	$B_{tor}$ , T	Heating/CD
NSTX	1.26	1	0.3 (5 s) 0.6 (1 s)	HHFW, 2 MW; NBI, 2.8 MW CHI →260 kA (500 kA)
MAST	1.3	1	0.6	NBI, 5 MW ECRH, 0.2 MW
GLOBUS-M	1.5	0.5	0.6	ICRH, 1.5 MW NBI, 1 MW; LHH, 1 MW
START	1.2	0.5	0.31	NBI, 1 MW ECRH, 0.2 MW
TST-2		0.09	0.3	HHFW, 0.3 MW
Pegasus	1.1	0.09	0.15	HHFW, 0.5 MW
HIT-II	1.5	0.02	0.3	CHI

#### 4. Auxiliary heating and current drive

Information about the heating and current drive (CD) methods which were used during the most recent experiments in major tokamaks and stellarators is presented in Tables II and III, respectively. There are many important results.

Negative ion based neutral beam heating used in JT-60U, not only makes it possible to simulate  $\alpha$ -particles interaction with the plasma, which was mentioned previously, but also makes it possible to control the power deposition profile. This provides the possibility to realize regimes with enhanced confinement and to drive a fully non-inductive current of 1.5 MA with an efficiency of up to  $\eta_{NB} = 1.5 \times 10^{19}$  A/W·m<sup>2</sup>. The development of a new grill for LH wave injection in Tore Supra increases its efficiency and creates a condition where the part of the power reaches the plasma core. This permits the LHCD efficiency to be increased and LHCD to be used for  $q(r)$  profile control in the plasma core. Internal transport barrier formation was the result of such a possibility.

TAB. II. HEATING AND CURRENT DRIVE IN TOKAMAKS

Tokamak	NBI, MW	ICR, MW	ECR, MW	LH, MW	Comments
JET	20	12	Will be (5)	7	$j(r)$ profile control; threefold ITB; NTM threshold and full stabilization; combination of different heating methods
DIII-D	20 Co/Cntr	FW, 3	110 GHz, 2.5		$j(r)$ profile control, ICR and ECR combination; Co- and Contr-CD; 75% of non-inductive current; full NTM stabilization
JT-60U	20+4 N-NB Co/Cntr    / $\perp$		11 GHz, 0.75, 2 s	2.2 GHz, 10	Negative ion based, $E=360$ keV; $T_i=10-20$ keV; non-inductive $I_p=1.5$ MA; $U_{loop}=0$ ; $j(r)$ profile control; ITB; full NTM stabilization
Tore Supra		ICRH, FW, 9.5	118 GHz, 0.4 (2.5)	3.7 GHz, 6	LHCD, 4 MW from 1 antenna; $I_{non-ind}=0.8$ MA, $U_{loop}=0$ ; $\Delta t=75$ s; $j(r)$ profile control, EITB
ASDEX-U	20; $\perp$ (Will be   )	FW, mode convers., 6	140 GHz, 1.6		$I_{ECCD}=350$ kA; $j(r)$ profile control; ITB with Co-CD and Contr-CD; MHD and NTM stabilization
TCV			83 GHz, 1.5; 118 GHz, 1		3-rd harmonic full absorpt.; $k=2.4$ , off-axis CD only; $I_{non-ind}=210$ kA $j(r)$ profile control; EITB ( $T_e(0)=14$ keV)
TEXTOR	4	ICRH, 32.2 MHz, 4.4	110 GHz, 0.3		RI-mode; high $n_e/n_{Gr}$ ; $j(r)$ profile control
T-10			140 GHz, 1.2		$j(r)$ profile control; ITB and H-mode; (double barrier). Plasma potential measurements. NTM investigation. Pellet injection mode
Alcator C-Mod		80 MHz, 5		4.6 GHz, 3	ICRF, ITB, H-mode in OH also. High $V_{  }$ rotation ( $\sim 50$ km/s); D-alpha-mode
Castor				0.05	Near-grill plasma investigation

TAB. II (continued)

Tokamak	NBI, MW	ICR, MW	ECR, MW	LH, MW	Comments
FTU		IBW 433 MHz, 0.35	140 GHz, 0.8	8 GHz, ~5	Synergy of LH and ECR→ECCD absorption at $B_{\parallel}$ higher than resonance; ITB; H-mode; pellet injection improved mode; specific distortion of $f_e(E)$ in low-E region; heat flux against $\nabla T$ ; tearing mode stabilization
JFT-2M	2×0.8 Co and Contr	FW, 200 MHz, 0.4	60 GHz, 0.5 (1)		FWCD; new «combine» antenna; H-mode study; plasma potential fluctuation measurements
TRIAM-1M				2.45 GHz, 0.05 2.8 GHz, 0.4	$j(r)$ profile control; long existence of the optimal profile; combination of different CD directions and waves with two frequencies for $j(r)$ formation; mode with enhanced $\eta_{CD}$ and improved confinement
HT-7		IBW, 30 MHz, 0.3		1	LHCD; $j(r)$ profile control; improved confinement; $n_{e,lim}$ ; ICR wall conditioning
COMPASS-D			60 GHz, 0.4	1.3 GHz, 1.5	H-mode threshold; high $\beta$ , Counter-ECCD on-axis, Co-LHCD off-axis; plasma rotation investigation
FT-2				0.1	$j(r)$ profile control; ITB
TUMAN-3M					OH H-mode; barrier formation by $j(r)$ perturbation

A high value of  $\eta_{LH} \approx 1 \times 10^{19}$  A/W·m<sup>2</sup> was found in LH experiments at TRIAM-1M. An unexpected effect of a sudden  $\eta_{LH}$  increase during fully non-inductive discharge start was found. Combination of two LH wave frequencies permitted good control of the  $q(r)$  profile.

In FTU the synergy between LH and ECR methods make it possible to obtain 70% absorption for the magnetic field, 45% higher than what is needed for the cold EC resonance. This effect appears due to absorption by the suprathermal electron tail induced by LHCD because of the relativistic Doppler effect.

In TCV, for the first time an experiment was performed with third harmonic X-polarized ECR power absorption in the plasma, previously heated by second harmonic X-mode ECR. This result opens the possibility to do experiments with a high density in tokamaks with low magnetic fields (1.5 T in this case).

An important result was achieved on W7-AS. ECR power density  $P=50$  W/cm<sup>3</sup>, leading to non-linear  $\eta_{ECCD}$  limitation, was obtained. Of course, this value is dependent on the plasma conditions, firstly on the plasma density, but the existence of such a limit is important for a future.

In previous years the main auxiliary heating power was used to heat ions. The special feature of Table II is the appearance of ECR heating/CD for many tokamaks. Owing to this, many devices obtained the possibility to control the current density profile, as this method permits heating or driving the current locally within the plasma (FIG. 3), so many experiments with MHD mode stabilization and internal transport barrier (ITB) formation were performed.

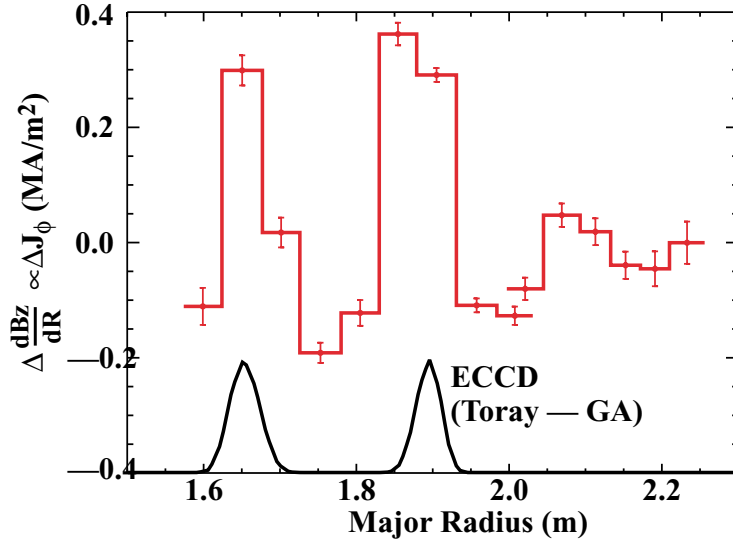


FIG. 3. DIII-D. The radial location of the ECCD from MSE measurements (red line) agrees well with calculations from TORAY-GA modeling (black).

TABLE III. HEATING AND CURRENT DRIVE IN STELLARATORS

Device	NBI, MW	ICR, MW	ECR, MW	Comments
W7-AS			140 GHz, 1.3	CD for current compensation, degradation of $\eta_{\text{ECCD}}$ for $P_{\text{EC}}=50 \text{ W/cm}^3$ ; enhancement of confinement time. Boundary island control by external coils; H-mode window in $\nu/2\pi$ space
LHD	4.2	26-38 MHz, 1.4	0.9	Long plasma pulse (68 s). Tokamak level of parameters; $\beta_t=2.4\%$ ( $B=1.3 \text{ T}$ ); H mode
TJ-2	3		53 GHz, 0.6	$T_e$ up to 2 keV; $\chi_e \approx 4 \text{ m}^2/\text{s}$ ; magnetic islands; internal and external E-barriers in rational surface regions
CHS			0.1	ITB barriers at rational surfaces; plasma potential $\Phi(r)$ measurements

## 5. Neoclassical tearing mode stabilization

The common opinion is that  $\beta_{\text{N lim}}$  is determined by neoclassical tearing mode (NTM) development. Experiments in this area are carried out at many tokamaks: JET, DIII-D, ASDEX-U, JT-60U, T-10, TCV, FTU and TFTR (previously).

In all experiments the soft  $\beta$  limit is found and the dependence of the threshold of NTM growth on the plasma parameters is investigated. Mainly the  $m/n=3/2$  mode attracts experimentalists. The most advanced experiments are performed at ASDEX-U, DIII-D and JT-60U, where attempts to stabilize these modes by ECRH/ECCD were made. It was shown that when the power is absorbed in some definite region inside the island, the fluctuation amplitude and the island dimension might be decreased and  $\beta_{\text{N lim}}$  increased up to the value that it had without this NTM island activity. Co-ECCD is better than heating only, and Counter-CD does not give the effect at all (DIII-D, FIG. 4). So the role of current redistribution was clearly demonstrated. The necessary position of the power deposition

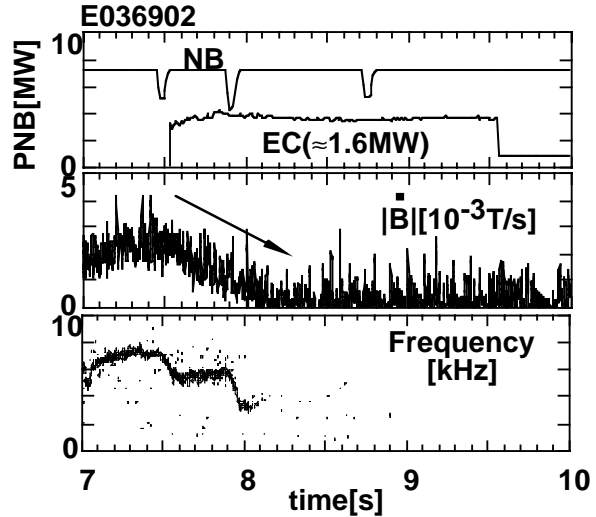
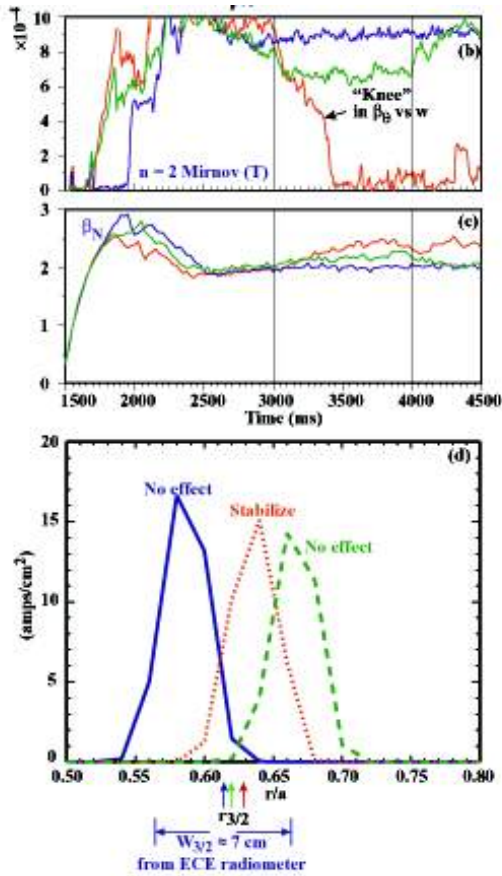


FIG. 4 (left). DIII-D. Stabilization of  $m=3/n=2$  NTM with ECCD; b) the  $n=2$  Mirnov coils show NTM stabilization (red curve); c)  $\beta_N$  recovers (red) for the stabilized case; d) the localized ECCD (TORAY-GA) stabilizes the NTM when applied at the proper radius (red). A  $B_T$  ramp-up was used to sweep the location of the ECCD. The thick vertical line shows the end of ECRH.

FIG. 5 (right). JT-60U. Suppression of the  $(m/n)=(3,2)$  neoclassical tearing mode by local ECCD on the mode resonant layer.

appears to be in a narrow region (less than the island width). So it is concluded that the dominant stabilizing effect is the generation of helical current in the island. A very important feature for the future is that  $P_{\text{ECCD}}/P_{\text{tot}}$  must be about 16% for total mode stabilization.

It is interesting that in the above-mentioned experiments with Co-CD, when  $P_{\text{ECR}}/P_{\text{tot}}$  was high enough, the instabilities did not reappear if ECR power was reduced after their total stabilization, or was even switched off (FIGS 4 and 5). It is also interesting that the attempt to stabilize NTM with the feedback system, using modulated ECR power, made no difference for the power-input position near O- or X-points of the island [1]. The same result was found for classical  $m=2$  mode stabilization in JFT-2M experiments some years ago. (Of course, the energy deposition profile in these experiments probably was not narrow enough to demonstrate the destabilization effect for ECR power deposition into the X-point.) In JET experiments the hard and soft  $\beta$  limits were investigated. It was shown that  $\beta$  degradation might be suspended by heavy gas puffing. All this shows that the change in the current density profile and therefore  $\Delta'$  criterion may be important. The plasma tendency to self-organization was seen many times; therefore one should expect that such a profile would be maintained during some time. It is not known from experiments, whether this stabilization will be steady state, or NTM will appear again after the current reconstruction time or sooner, but even in the latter case the necessary power will be used only periodically and it will be significantly less than 16% of  $P_{\text{tot}}$ . This should be good for reactor parameter regulation.

The fact that  $\beta$  does not increase after stabilization to the value at the discharge beginning (see FIG. 4) perhaps means that the  $m/n=3/2$  mode is not the only important mode, so more investigations (probably for the  $m/n=2/1$  mode) are needed.

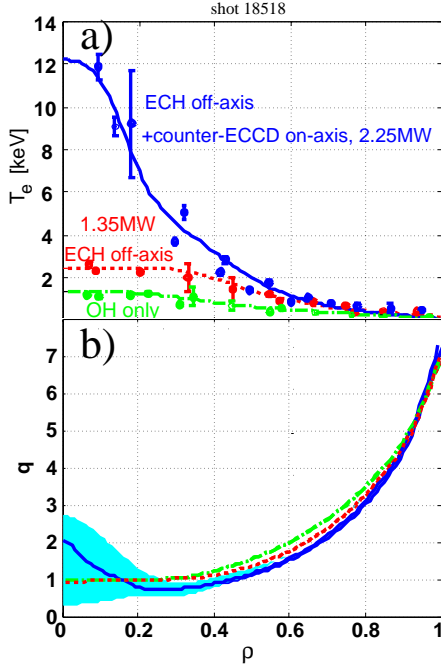


FIG. 6. TCV. (a) Electron temperature profiles measured by Thomson scattering along a vertical chord for three shots: red – off-axis ECH (at a normalized minor radius  $\rho_h = 0.37$ ), blue – 1.35 MW off-axis ECH and 0.9 MW on-axis counter-ECCD, and green – OH only. (b) Calculated  $q$  profiles. ECR power deposition is taken from the TORAY code.

## 6. ITB with negative or low shear

The availability of a wider range of auxiliary heating/CD methods stimulated many experiments with ITB formation on a number of tokamaks and they have made exiting progress.

At the beginning these regimes were organized by NBI during the plasma current ramp-up phase. It was found that only an **Ion ITB** could be formed. But soon, in experiments where the electron component received enough heating power, electron internal transport barriers (**E-ITB**) were also found. Now, when many tokamaks use the ECRH/ECRCD and lower hybrid (LH) methods, impressive results in this area are being reached (see the results of ASDEX-U, FTU, DIII-D, TCV and T-10, etc.). For example, in TCV a high increase of the central  $T_e$  was seen under on-axis counter-CD (FIG. 6).

The appearance of a region of low transport coefficients for ions is explained by the appearance of shear of drift rotation,  $\omega_{E \times B}$ , which stabilizes the ion temperature gradient mode (ITG) or other modes that determine ion confinement:

$$|\omega_{E \times B}| = \left| \frac{RB_\theta^2}{B_\phi} \frac{\partial}{\partial \psi} \frac{E_r}{B_\theta} \right| > \gamma_{lin, max}$$

Here  $B_\theta$  and  $B_\phi$  are the toroidal and poloidal magnetic fields,  $\Psi$  is the poloidal magnetic flux,  $R$  is the major radius,  $E_r$  is the radial electric field and  $\gamma_{lin, max}$  is the linear increment of the most dangerous instability. The same explanation is used for the plasma edge barrier, L-H transition. NBI provides the toroidal rotation momentum. In DIII-D, JT-60U and ASDEX-U the role of this momentum was investigated using different directions of NBI and some effects were observed.

However, in many experiments ITB formation takes place without any momentum injection (ICRH, LHH, ECRH, etc.) and rotation shear also arises. In all experiments with ITB formation the region of low magnetic shear is needed, but it was found that a negative shear region is not needed. The place of barrier formation is always near  $q_{min}$  or  $q_{flat}$ , so that  $dq/dr$  is low and the  $q$  value is near the resonance:  $q=1; 1.5; 2 \dots$  and so on (FIGS 7, 8).



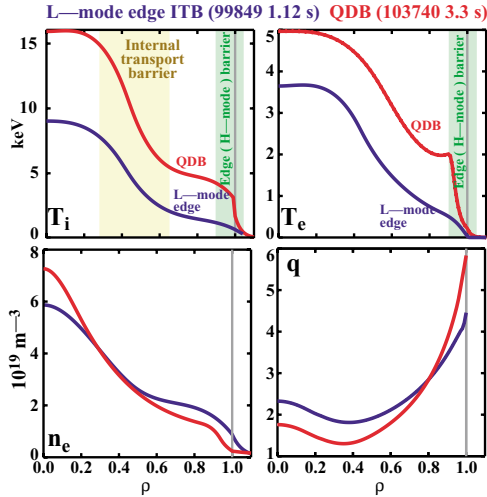


FIG. 7. DIII-D. Single and double barrier formation. The internal barrier takes place near the  $q(r)_{\min}$  region in both cases.

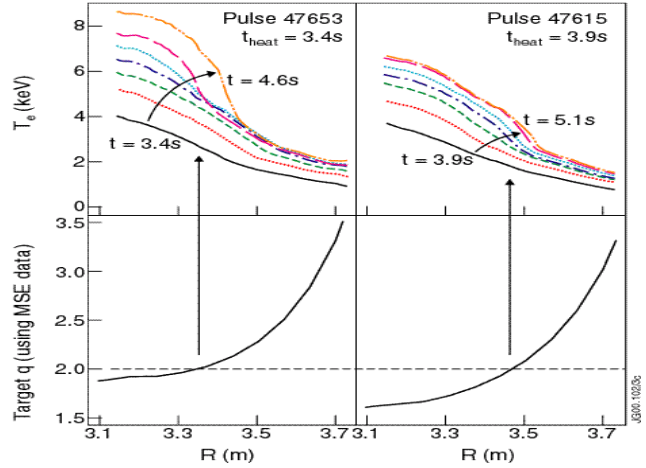


FIG. 8. JET. An ITB may be formed in experiments without negative shear. The temporal evolution of the ITB (from ECE) for various  $q(r)$  profiles is shown.

In FIG. 8 the dynamics of ITB formation is shown. The increase of the central  $T_e$  must change  $q(r)$  and position of  $q=2$  should be shifted outward. This may be the reason for some increase of the barrier radius during ITB formation. Probably the high pressure gradient also plays an important role in ITB formation.

So we see that the current density distribution and hence  $T_e(r)$  are important factors for ITB formation. In some cases, changes in  $q_{\min}$  near the rational value lead to loss of MHD stability and barrier existence (ASDEX-U).

There is an opinion that the physics of Ion ITB and of E-ITB are quite different, because the shear of rotation rate for stabilization of ion and electron instabilities is very different. But it seems that the *heart* of the ITB phenomenon is the  $q$  profile, and it must be the same for both electron and ion barrier formation.

**What is the reason for the appearance of the rotation shear?** Some theories presented at the conference give different variants of rotation shear appearance. These are: loss of ions from banana orbits, specific effects connected with ICR heating, turbulence self-stabilization and so on. Perhaps all of these suggestions may be realized in the plasma, but the phenomenon of transport barrier formation is so regular that we have to expect some robust common reason. Let us look at the experiments. In T-10 the evolution of plasma potential distribution during ITB formation was measured directly (FIG. 9). A deep narrow potential well is seen in the barrier region during its formation. (The same is true for the edge barrier.) The simplest explanation is that the balance between electron and ion fluxes, leading to ambipolarity, is broken owing either to ion flux increase or to electron flux decrease in the narrow region. As in the same experiment the measured ion confinement increases during ITB formation, we have to conclude that the electron transport decreases. The appearance of the potential well leads to the rise of a very strong rotation shear. The rotation rate even changes its sign in the barrier region.

**Why does low shear in the vicinity of the rational surface distort the balance of fluxes?** The question is still open. The theory presented at the conference predicts that the ETG (electron transport gradient) mode will be stabilized in the region with low shear and high

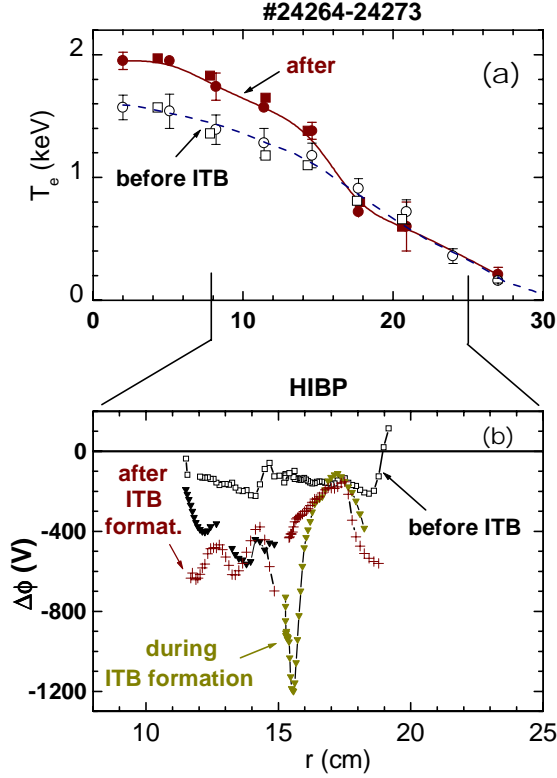


FIG. 9. T-10. a) The electron temperature profile from Thomson scattering (circles) and ECE (squares); b) profiles of the relative (to the time long before the transition) potential well  $\Delta\Phi(r)$  just before, during and after ITB formation.

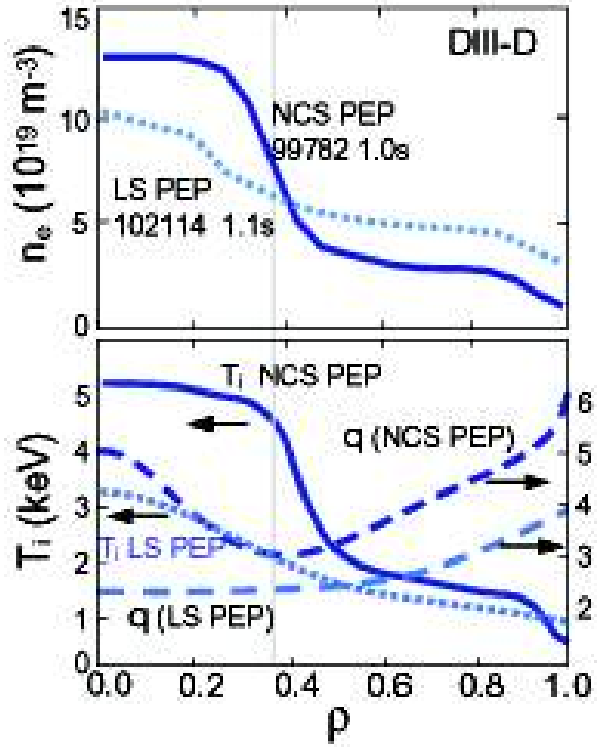


FIG. 10. DIII-D. Profiles of  $n_e$ ,  $T_i$  and  $q$  for pellet-induced ITB (NCS PEP) and low-shear ITB (LS PEP) plasmas. The strong gradients for the NCS PEP are just inside the minimum in the  $q$  profile (vertical line).

pressure gradient, but it does not bound with the rational surface – the important feature of the experimental results.

Another surprising phenomenon is found in T-10, DIII-D and JET experiments, the simultaneous formation of two (and even three) barriers: ITB and external, H-mode type. (Perhaps the same effect is seen in ASDEX-U “Enhancement H mode”.) This poses new questions for explanation of H-mode formation. Is it an interaction between different resonance surfaces? A similar phenomenon has been registered in JT-60U: the strong ELM event has its quick response at the ITB region.

Of course, it is desirable to have a more or less common explanation for all kinds of modes with enhanced confinement.

Different methods of obtaining the enhanced confinement modes exist: supershot, RI-mode, high ion temperature mode, mode with pellet injection and so on. At present the last named is very popular.

**Pellet injection.** Experiments with pellet injection during auxiliary heating are carried in many tokamaks: DIII-D, JET, ASDEX, FTU and T-10. A promising new method of pellet injection from the high magnetic field side realizes a deeper particle penetration into the plasma. Comparison of experiments with different directions of injection (high and low field side, vertical) shows that in all cases it is possible to form an ITB, but deeper pellet penetration in the case of the high field side injection leads to steeper barrier gradients. Barriers for all parameters ( $T_i$ ,  $T_e$ ,  $n_e$ ) are realized. In FTU experiments, where the magnetic

field is high (about 5 T), the barrier after the pellet injection was formed without any auxiliary heating, seemingly because of the high current density and so the high OH power. The ITB may be formed with the negative, flat or slightly positive shear. But the “foot” of the ITB is always situated in the region of low shear, (*FIG. 10*). In these experiments again two barriers, one inside and another at the edge (H-mode), exist simultaneously.

**RI mode.** Many experiments show that with the injection of heavy gas (Ne or Ar), better confinement can be obtained in different modes of tokamak operation. Such gas puffing leads to cooling at the plasma edge (light gas puffing does not give the same effect), so this is a way to redistribute  $T_e$  and hence  $j(r)$  at the edge. There is not enough information about the profile, which is organized when the plasma confinement improves. Does the internal barrier exist in the RI mode?

It is important to note that an ITB-like formation has been found not only in tokamaks. An effect similar to ITB was seen in the reversed field pinch MST. In currentless stellarators TJ-2 and CHS, ITB formation was registered near resonance surfaces. The H-mode configuration exists there also (see experiments in W7-AX, where  $\iota/2\pi$  regions exist for H-mode operation). In CHS experiments two barriers, one with  $\nabla T_e$  in the core and another with  $\nabla n_e$  at the edge, are formed.

**Does the heat pinch exist?** This question has arisen many times during the last several years, and has not been solved fully yet. Two reports from RTP and FTU pose this question again. The name “heat pinch” is not correct. Really we mean non-diffusion heat flux, which in some specific cases may pass against the temperature gradient. Just such results were reported in these two papers.

Perhaps we have missed some fundamental feature of magnetic confinement systems, the understanding of which could help us greatly in high performance tokamak organization. The plasma, with its tendency to self-organization, in many cases helps us to obtain better parameters.

It seems that the time of scalings is over. Instead of scalings, now we need to understand the physics of processes in the plasma. This will allow us to predict plasma behavior more correctly.

## References

- [1] ZOHN, H., et al., "Experiments on neoclassical tearing mode stabilization by ECCD in ASDEX Upgrade", *Nucl. Fusion* **39** (1999) 577.

## Acknowledgement

The author thanks all her colleagues whose papers have provided the basis for this review, and Dr. S. Lysenko and Ms. M. Spak for assistance in the manuscript preparation.